

Rapid Commun. Mass Spectrom. 2015, 29, 269–282  
(wileyonlinelibrary.com) DOI: 10.1002/rcm.7102

# Isotope fractionation factors controlling isotopocule signatures of soil-emitted N<sub>2</sub>O produced by denitrification processes of various rates

Dominika Lewicka-Szczebak<sup>1,2\*</sup>, Reinhard Well<sup>1</sup>, Roland Bol<sup>3</sup>, Andrew S. Gregory<sup>4</sup>, G. Peter Matthews<sup>5</sup>, Tom Misselbrook<sup>6</sup>, W. Richard Whalley<sup>4</sup> and Laura M. Cardenas<sup>6</sup>

<sup>1</sup>Thünen Institute of Climate-Smart Agriculture, Federal Research Institute for Rural Areas, Forestry and Fisheries, Bundesallee 50, D-38116 Braunschweig, Germany

<sup>2</sup>Institute of Geological Sciences, University of Wrocław, Cybulskiego 30, PL-50-205 Wrocław, Poland

<sup>3</sup>Forschungszentrum Jülich IBG-3, Wilhelm-Johnen-Straße, 52428 Jülich, Germany

<sup>4</sup>Rothamsted Research, Harpenden AL5 2JQ, UK

<sup>5</sup>Faculty of Science & Environment, University of Plymouth, Plymouth PL4 8AA, UK

<sup>6</sup>Rothamsted Research, North Wyke, Okehampton EX20 2SB, UK

**RATIONALE:** This study aimed (i) to determine the isotopic fractionation factors associated with N<sub>2</sub>O production and reduction during soil denitrification and (ii) to help specify the factors controlling the magnitude of the isotope effects. For the first time the isotope effects of denitrification were determined in an experiment under oxic atmosphere and using a novel approach where N<sub>2</sub>O production and reduction occurred simultaneously.

**METHODS:** Soil incubations were performed under a He/O<sub>2</sub> atmosphere and the denitrification product ratio [N<sub>2</sub>O/(N<sub>2</sub> + N<sub>2</sub>O)] was determined by direct measurement of N<sub>2</sub> and N<sub>2</sub>O fluxes. N<sub>2</sub>O isotopocules were analyzed by mass spectrometry to determine δ<sup>18</sup>O, δ<sup>15</sup>N and <sup>15</sup>N site preference within the linear N<sub>2</sub>O molecule (SP). An isotopic model was applied for the simultaneous determination of net isotope effects (η) of both N<sub>2</sub>O production and reduction, taking into account emissions from two distinct soil pools.

**RESULTS:** A clear relationship was observed between <sup>15</sup>N and <sup>18</sup>O isotope effects during N<sub>2</sub>O production and denitrification rates. For N<sub>2</sub>O reduction, diverse isotope effects were observed for the two distinct soil pools characterized by different product ratios. For moderate product ratios (from 0.1 to 1.0) the range of isotope effects given by previous studies was confirmed and refined, whereas for very low product ratios (below 0.1) the net isotope effects were much smaller.

**CONCLUSIONS:** The fractionation factors associated with denitrification, determined under oxic incubation, are similar to the factors previously determined under anoxic conditions, hence potentially applicable for field studies. However, it was shown that the η<sup>18</sup>O/η<sup>15</sup>N ratios, previously accepted as typical for N<sub>2</sub>O reduction processes (i.e., higher than 2), are not valid for all conditions. Copyright © 2014 John Wiley & Sons, Ltd.

Denitrification is an anaerobic microbial process of successive reduction of nitrate (NO<sub>3</sub><sup>-</sup>) to nitrous oxide (N<sub>2</sub>O) and dinitrogen (N<sub>2</sub>).<sup>[1]</sup> This process can be significantly enhanced by the addition of nitrogen fertilizers to agricultural soils, resulting in enhanced loss of mineral N and intensified N<sub>2</sub>O emissions,<sup>[2]</sup> which significantly contribute to global warming and stratospheric ozone depletion.<sup>[3,4]</sup> Hence, the ability to quantify this process is important for developing fertilizing strategies mitigating the microbial consumption of N fertilizers and reducing their environmental impacts. However, the loss of the final denitrification product, N<sub>2</sub>, cannot be directly measured in field conditions due to high atmospheric background. Although an inert gas, N<sub>2</sub>

is important in understanding the dynamics of the entire denitrification process and it can thus be responsible for significant N losses from the ecosystem. Laboratory studies showed that the product ratio of denitrification [N<sub>2</sub>O/(N<sub>2</sub> + N<sub>2</sub>O)] can vary in a very wide range from 0 to 0.94,<sup>[5–7]</sup> but the controls of these variations are not yet well defined. Therefore, development of methods enabling determination of the above-mentioned product ratio under field conditions is needed.

Stable isotopic analyses of N<sub>2</sub>O by mass spectrometry (MS) can potentially help to quantify the contribution of N<sub>2</sub>O reduction to N<sub>2</sub>. Current MS techniques allow us to determine the isotopic composition of N<sub>2</sub>O (δ<sup>15</sup>N and δ<sup>18</sup>O values), and simultaneously the <sup>15</sup>N site preference (SP) of the linear N<sub>2</sub>O molecule.<sup>[8,9]</sup> All these three N<sub>2</sub>O isotopocule signatures (δ<sup>15</sup>N, δ<sup>18</sup>O, and SP values) are altered during the N<sub>2</sub>O reduction process and the magnitude of the observed change depends largely on the product ratio.<sup>[10–13]</sup> However, to determine the product ratio from the isotopic signature of

\* Correspondence to: D. Lewicka-Szczebak, Thünen Institute of Climate-Smart Agriculture, Federal Research Institute for Rural Areas, Forestry and Fisheries, Bundesallee 50, D-38116 Braunschweig, Germany.  
E-mail: dominika.lewicka-szczebak@ti.bund.de

the residual  $\text{N}_2\text{O}$ , the characteristic isotopic signatures for the initially produced  $\text{N}_2\text{O}$  and the characteristic fractionation factors associated with  $\text{N}_2\text{O}$  reduction must be known. The  $\delta^{15}\text{N}$  and  $\delta^{18}\text{O}$  values of the produced  $\text{N}_2\text{O}$  depend on the isotopic signatures of the  $\text{N}_2\text{O}$  precursors ( $\text{NO}_3^-$  and  $\text{H}_2\text{O}$ ) and on the transformation pathways (e.g., various isotope effects for nitrification and denitrification<sup>[14,15]</sup>). The SP values, however, are independent of the precursors, but differ according to different pathways (e.g., nitrification and denitrification<sup>[16]</sup>) and different microbial communities involved in the  $\text{N}_2\text{O}$  production (e.g., bacterial and fungal denitrification<sup>[17,18]</sup>). Our current knowledge about the fractionation factors associated with various  $\text{N}_2\text{O}$  production pathways is based mainly on pure culture studies.<sup>[16,18–21]</sup> A few laboratory soil incubations with natural soil communities have also been performed, which were targeted at one particular process, such as nitrification<sup>[14,15,22]</sup> or denitrification,<sup>[14,23–26]</sup> by using the required soil moisture and headspace atmosphere (oxic or anoxic). It is also possible to investigate one particular process after inhibition or exclusion of the accompanying processes by using (i) acetylene to inhibit  $\text{N}_2\text{O}$  reduction<sup>[11,26]</sup> or (ii)  $\text{NO}_3^-$ -free soil to exclude  $\text{N}_2\text{O}$  production.<sup>[10–13,27]</sup>

But are the fractionation factors determined for artificially regulated processes transferable to natural field conditions? Only recently, the first attempts have been made to apply isotopic signatures of soil-emitted  $\text{N}_2\text{O}$  to distinguish production pathways and microbial communities involved in  $\text{N}_2\text{O}$  production and to quantify  $\text{N}_2\text{O}$  reduction under field conditions.<sup>[28–31]</sup> However, due to uncertainties on the actual fractionation factors, so far only very rough flux estimations have been made. Hence, there is still a gap between information on the fractionation factors obtained in targeted laboratory incubations and that applicable in field studies, namely, experimental studies under conditions mostly similar to natural field environment are lacking. Only recently has it been shown that the magnitude of fractionation factors of  $\text{N}_2\text{O}$  reduction strongly depends on the experimental approach, i.e., for dynamic conditions the isotope effects are significantly lower than for static experiments, i.e., those in which  $\text{N}_2\text{O}$  is accumulated in the headspace.<sup>[24]</sup> Similarly, it is known that the process rate has an impact on the magnitude of isotope effects.<sup>[10,27,32]</sup> Nevertheless, all these types of experiments that have been used until now to determine denitrification isotope effects were conducted under anoxic atmospheres. It can be assumed that the results may be different from those under oxic conditions as a result of very different dynamics, e.g., much higher denitrification rates in anoxic atmosphere.

Here we present the first laboratory study for the determination of isotope effects associated with denitrification under oxic atmosphere. We applied an enhanced experimental approach allowing for simultaneous  $\text{N}_2\text{O}$  production and reduction within the same soil incubation vessel.<sup>[24]</sup> Such an approach has a clear advantage over experiments which separate these two reaction steps since, under natural conditions, production and reduction occur simultaneously within the same soil microsites or even within the same microbial cells. However, in such an approach we are dealing with two unknown fractionation factors. They can be successfully determined by applying iterative modelling if the product ratio is known and it changes in

time.<sup>[24]</sup> Hence, an independent method for product ratio determination is necessary. Of the available methods, only direct  $\text{N}_2$ -flux measurement enables quantification of both  $\text{N}_2\text{O}$  production and reduction, with simultaneous analysis of the associated isotope effects, within a single soil incubation vessel. This requires the incubation in artificial  $\text{N}_2$ -free atmosphere and precise measurements of  $\text{N}_2$  fluxes. In this study we therefore performed incubations in an  $\text{He}/\text{O}_2$  atmosphere in which  $\text{N}_2$  and  $\text{N}_2\text{O}$  fluxes were measured directly. Moreover, treatments with various water contents were applied to obtain various denitrification rates. The results of this study should help to better define isotope effects applicable for natural conditions and, in consequence, enable more precise flux estimations in field studies.

The gas flux measurements and  $\text{N}_2\text{O}$  isotopic signatures from these incubations formed part of a separate study (unpublished results). Here we present a modelling approach based on these experimental data suitable to evaluate the isotope effects associated with denitrification processes at various rates. The first objective of our study was to determine fractionation factors of denitrification  $\text{N}_2\text{O}$  production and reduction using a novel, more field-like, approach under oxic conditions. The second objective was to elucidate the specific factors controlling the magnitude and variability of the isotope effects, which could possibly provide an explanation for the wide range of the fractionation factors reported by previous studies and allow for better assessment of the factors applicable for field conditions.

## EXPERIMENTAL

### Set-up

An agricultural silty clay loam soil under grassland management was collected from a location adjacent to a long-term ley-arable experiment at Rothamsted Research in Hertfordshire, UK (Highfield, further details in, e.g., Gregory, *et al.*<sup>[33]</sup>). The soil cores were prepared to different water saturation treatments, based on water-filled pore space (WFPS), of which the following three treatments were used in our modelling exercise:

- 100% WFPS; micropores saturated, macropores saturated, further referred to as 'SAT';
- 94% WFPS: micropores saturated, macropores half-saturated, further referred to as 'HALFSAT';
- 85% WFPS: micropores saturated, macropores unsaturated, further referred to as 'UNSAT';

Each water treatment was replicated in three vessels. An amendment solution equivalent to  $75 \text{ kg N ha}^{-1}$  and  $400 \text{ kg C ha}^{-1}$  was applied as a one-point injection of a 5 mL solution containing  $\text{KNO}_3$  and glucose on the top of the soil. The vessels were continuously flushed with a  $\text{He}/\text{O}_2$  mixture (21%  $\text{O}_2$ ) with a flow rate of  $10 \text{ mL min}^{-1}$ . The incubation lasted 12 days under controlled temperature ( $20^\circ \text{C}$ ). At the end of the incubation the initial soil moisture had decreased by 20, 10 and 7% for SAT, HALFSAT and UNSAT treatment, respectively. The soil incubation procedure was similar to the one used in previous studies.<sup>[34,35]</sup>

## Measurements

The N<sub>2</sub>O and N<sub>2</sub> fluxes were analyzed continuously in ca. 2-h intervals. The effluent gas sample was split to analyze N<sub>2</sub>O and N<sub>2</sub>. N<sub>2</sub>O was separated on a stainless steel packed column (2 m long, 4 mm bore) filled with 'Porapak Q' (80–100 mesh) and quantified by Electron Capture Detection (ECD). The detection limit was equivalent to 2.3 g N ha<sup>-1</sup> day<sup>-1</sup>. N<sub>2</sub> was separated on a PLOT column (30 m long 0.53 mm i.d.) and quantified by He Ionisation Detection (HID). The detection limit was 9.6 g N ha<sup>-1</sup> day<sup>-1</sup>.

The samples for N<sub>2</sub>O isotopocule analysis were collected daily in 115 mL sealed serum bottles connected to the end of the chamber vents by a Teflon tube and vented to the atmosphere through a needle to maintain flow through the experimental system. N<sub>2</sub>O samples were analyzed using a Delta V isotope ratio mass spectrometer (Thermo Scientific, Bremen, Germany) coupled to an automatic preparation system (Precon+Trace GC Isolink; Thermo Scientific). N<sub>2</sub>O was separated from CO<sub>2</sub> with an Ascarite trap, cryogenically pre-concentrated, and chromatographically purified. In the mass spectrometer, the N<sub>2</sub>O isotopocule signatures were determined by measuring *m/z* 44, 45, and 46 of intact N<sub>2</sub>O<sup>+</sup> molecular ions as well as *m/z* 30 and 31 of NO<sup>+</sup> fragment ions. This allows the determination of the average δ<sup>15</sup>N (δ<sup>15</sup>N<sub>bulk</sub>), δ<sup>15</sup>N<sub>α</sub> (δ<sup>15</sup>N of the central N position of the N<sub>2</sub>O molecule), and δ<sup>18</sup>O values.<sup>[9]</sup> δ<sup>15</sup>N<sub>β</sub> (the δ<sup>15</sup>N value of the peripheral N position of the N<sub>2</sub>O molecule) is calculated from δ<sup>15</sup>N<sub>bulk</sub> = (δ<sup>15</sup>N<sub>α</sub> + δ<sup>15</sup>N<sub>β</sub>)/2. The <sup>15</sup>N site preference (SP) is defined as SP = δ<sup>15</sup>N<sub>α</sub> - δ<sup>15</sup>N<sub>β</sub>. The scrambling factor and <sup>17</sup>O-correction have been taken into account.<sup>[36]</sup> Pure N<sub>2</sub>O was used as the reference gas and this was analyzed for isotopocule signatures in the laboratory of the Tokyo Institute of Technology using the previously reported calibration procedures.<sup>[9,37]</sup> All isotopic signatures are expressed as ‰ deviation from the <sup>15</sup>N/<sup>14</sup>N and <sup>18</sup>O/<sup>16</sup>O ratios of the reference materials (i.e., atmospheric N<sub>2</sub> and Vienna Standard Mean Ocean Water (V-SMOW), respectively). The analytical precision determined as standard deviation (1σ) of the internal standards for measurements of the δ<sup>15</sup>N, δ<sup>18</sup>O, and SP values was below 0.2‰, 0.2‰, and 0.8‰, respectively.

## Calculation methods

The experimentally determined isotope effects represent the overall isotope effects, resulting from both physical and enzymatic fractionation, and are called the Net Isotope Effects (NIE), denoted by η.<sup>[24,32,38]</sup> The η values are given in the relation product-to-substrate, hence negative η values indicate product depletion in heavy isotopes. In such a case the more negative values indicate larger NIE (higher difference between product and substrate), whereas values closer to 0 indicate smaller NIE (lower difference). The positive values indicate an inverse effect, i.e., product enrichment in heavy isotopes.

The η values were calculated based on Rayleigh distillation equation:<sup>[39]</sup>

$$\frac{\delta_S + 1000}{\delta_{S0} + 1000} = f^{\frac{\eta_{p-s}}{1000}} \quad (1)$$

where δ<sub>S</sub> is the isotopic signature of remaining substrate in the particular point of the process; δ<sub>S0</sub> the initial isotopic signature of substrate; *f* the remaining unreacted fraction; and η<sub>p-s</sub> the NIE between product and substrate.

## N isotope effect of N<sub>2</sub>O production

During the progress of denitrification the substrate is continuously enriched in <sup>15</sup>N. Thus, to calculate the isotopic signature of the product, N<sub>2</sub>O, the isotopic signature of the remaining substrate, nitrate, must be calculated according to Eqn. (1), where: δ<sub>S</sub> is the isotopic signature of remaining nitrate (δ<sup>15</sup>N<sub>NO<sub>3</sub>-r</sub>); δ<sub>S0</sub> the isotopic signature of initial nitrate (δ<sup>15</sup>N<sub>NO<sub>3</sub>-i</sub>), i.e., fertilizer or soil nitrate. In this study these values were not determined, but adopted from literature data.<sup>[40,41]</sup>

$$\delta^{15}\text{N}_{\text{fertilizer NO}_3^-} = 0\text{‰} \text{ and } \delta^{15}\text{N}_{\text{soil NO}_3^-} = 10\text{‰}.$$

The uncertainty resulting from this simplification was estimated using the sensitivity tests presented later (see section 'Model construction'). *f*, the fraction of unreduced nitrate N, was calculated by subtracting the initial nitrate concentration and the cumulative N loss as denitrification products (N<sub>2</sub> + N<sub>2</sub>O) for each time step of the process:

$$f = (\text{N}_{\text{NO}_3^-} - \text{N}_{\text{N}_2 + \text{N}_2\text{O}}) / \text{N}_{\text{NO}_3^-} \quad (2)$$

It was assumed that the NO and NO<sub>2</sub><sup>-</sup> pools are negligible in the overall N balance, as these are very reactive intermediate products undergoing fast further reduction. η<sub>p-s</sub> is the NIE of N<sub>2</sub>O production referred to as η<sub>N<sub>2</sub>O-NO<sub>3</sub></sub>.

Having determined the δ<sup>15</sup>N<sub>NO<sub>3</sub>-r</sub> (remaining nitrate) value, the δ<sup>15</sup>N<sub>N<sub>2</sub>O-p</sub> (instantaneously produced N<sub>2</sub>O) value was calculated as:

$$\delta^{15}\text{N}_{\text{N}_2\text{O-p}} \cong \delta^{15}\text{N}_{\text{NO}_3\text{-r}} + \eta^{15}\text{N}_{\text{N}_2\text{O-NO}_3} \quad (3)$$

## O isotope effect of N<sub>2</sub>O production

The δ<sup>18</sup>O value of the produced N<sub>2</sub>O is mainly governed by the exchange of O-isotopes with soil water<sup>[24,42,43]</sup> and therefore the δ<sup>18</sup>O value of the remaining nitrate can actually be neglected. In such a case it is most appropriate to accept the δ<sup>18</sup>O value of soil water (δ<sup>18</sup>O<sub>H<sub>2</sub>O</sub>) as a substrate of the produced N<sub>2</sub>O (δ<sup>18</sup>O<sub>N<sub>2</sub>O-p</sub>). Since soil water is an almost infinite reservoir, there is no detectable substrate fractionation. Hence, the η<sub>N<sub>2</sub>O-H<sub>2</sub>O</sub> is calculated as:

$$\delta^{18}\text{O}_{\text{N}_2\text{O-p}} \cong \delta^{18}\text{O}_{\text{H}_2\text{O}} + \eta^{18}\text{O}_{\text{N}_2\text{O-H}_2\text{O}} \quad (4)$$

The δ<sup>18</sup>O<sub>H<sub>2</sub>O</sub> value was not determined, but this value can be quite well estimated based on the mean annual precipitation in the region. This value was adopted from the GNIP (Global Network for Isotopes in Precipitation) database<sup>[44]</sup> for the nearest precipitation monitoring station: Wallingford (GNIP code: 365302), where the annual mean δ<sup>18</sup>O value was -6.7‰.

## SP of produced N<sub>2</sub>O

The SP of the produced N<sub>2</sub>O is mainly governed by the species contribution in the active soil microbial community<sup>[18,21]</sup> and is independent of the precursor isotopic signature. Hence, the SP value of the produced N<sub>2</sub>O (SP<sub>N<sub>2</sub>O-p</sub>) represents the typical ηSP values for the particular process:

$$\text{SP}_{\text{N}_2\text{O-p}} = \eta \text{SP}_{\text{N}_2\text{O-NO}_3} \quad (5)$$

We have assumed that the microbial community does not change significantly during the experiment; thus, the SP of the produced  $N_2O$  was assumed to be stable.

### $N_2O$ reduction

The isotopic signature of the remaining  $N_2O$  was calculated according to Eqn. (1), where  $\delta_S$  is the isotopic signature of the remaining unreduced  $N_2O$  ( $\delta_{N_2O-r}$ );  $\delta_{S0}$  the isotopic signature of the instantaneously produced  $N_2O$  ( $\delta_{N_2O-p}$  calculated from Eqns. (3), (4), (5));  $f$  the fraction of unreduced  $N_2O$  calculated based on direct measurements of  $N_2O$  and  $N_2$  flux, i.e., the product ratio ( $N_2O/(N_2O + N_2)$ ); and  $\eta_{P-S}$  NIE of  $N_2O$  reduction referred to as  $\eta_{N_2-N_2O}$ .

### Model construction

The calculated  $\delta_{N_2O-r}$  values are further referred to as the modelled  $N_2O$  isotopic signatures and these are compared with the measured  $N_2O$  isotopic signatures. The iterative calculations were performed using the Microsoft Excel Solver tool applying the simplex method.<sup>[45,46]</sup> This method was compared with the Markov Chain Monte Carlo modelling approach and provided identical results.<sup>[24]</sup>

### Determination of emission pattern – Step 1

Due to the addition of the amendment solution during the experiment on the soil surface, the distribution of substrates was not homogenous within the incubated soils. Experiments of a similar set-up were previously carried out by Cardenas *et al.*,<sup>[35]</sup> Mejjida *et al.*,<sup>[47]</sup> and Bergstermann *et al.*<sup>[34]</sup> In all those studies, it has been suggested that the  $N_2O$  emissions originated from multiple pools. Similarly, in this experiment the observed variations in isotopic signatures cannot be explained by emission from one well-mixed pool. Therefore, we adopted a two-pool model for our simulations. Pool 1 represents the soil volume reached by the amendment solution, where the N flux originates from the added fertilizer, whereas Pool 2 represents the amendment-free soil, where the N flux originates from soil nitrates, present before or added through mineralization. The division of fluxes into these two pools was made according to the following assumptions: (i) before amendment application emissions are only due to Pool 2, (ii) after amendment application any increase in  $N_2O + N_2$  flux originates from Pool 1, and (iii) after extinction of the whole N of Pool 1 the flux must originate from Pool 2. However, after the extinction of N in Pool 1, quite high  $N_2 + N_2O$  emissions are still detected, and they cannot suddenly originate from another pool. This is probably due to the continuous mineralization of organic matter, which adds N available for denitrification. Hence, it is reasonable to assume that during the first emission peak, originating mainly from Pool 1, a small but increasing admixture of Pool 2 also occurs. The contribution of this admixture was fitted assuming an exponential increase of Pool 2 emission to finally reach the emission observed after the extinction of Pool 1 (see Fig. 1 and Appendix 1, Supporting Information). We observed quite similar dynamics for all the vessels, i.e., the first two or three sampling points after amendment addition showed a very high  $N_2O + N_2$  flux and a continuous enrichment in  $^{15}N$ . Then we observed a sudden drop in the  $N_2O + N_2$  flux as well

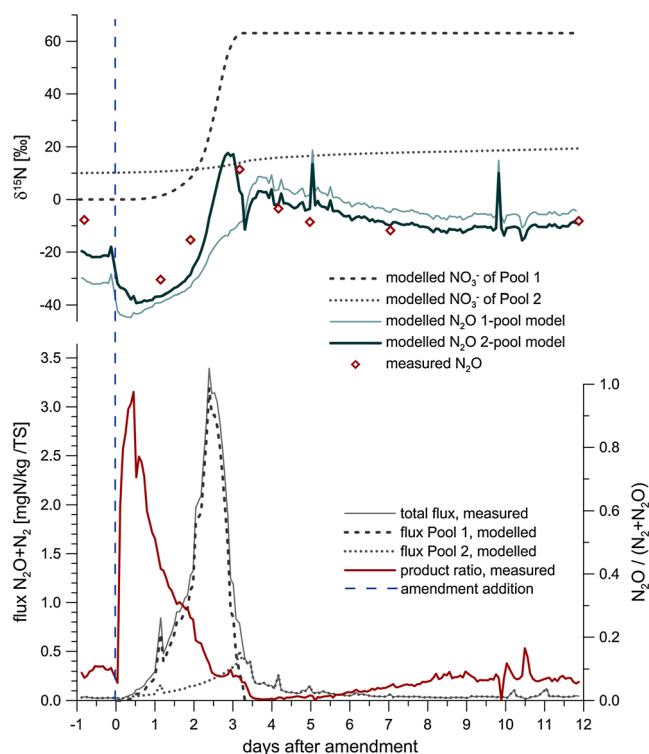


**Figure 1.** Measured total  $N_2 + N_2O$  flux with division into pools according to the model assumptions and the measured product ratio  $N_2O/(N_2 + N_2O)$  of the total flux (lower graph) with comparison of measured and modelled  $\delta^{15}N$  values of the emitted  $N_2O$  and of the residual  $NO_3^-$  (upper graph). Data for one sample vessel (V2 – HALFSAT treatment) are shown. TS – time step = 1 h 40 min.

as in the  $\delta^{15}N_{N_2O}$  value with quite a stable low flux and stable  $\delta^{15}N_{N_2O}$  values afterwards (Appendix 2, Supporting Information). Our assumed division into two pools enabled us to obtain very good agreement between the modelled and measured  $\delta^{15}N_{N_2O}$  values (Fig. 1).

### Determination of $\eta_{N_2O-NO_3}$ – Step 2

We are dealing with two unknown isotope effects:  $\eta_{N_2O-NO_3}$  – NIE associated with the  $N_2O$  production step and  $\eta_{N_2-N_2O}$  – NIE associated with the  $N_2O$  reduction step. Moreover, in the two emission pools we observe very different reaction rates for production and reduction (Fig. 1): Pool 1 is characterized by a very high production rate, and high product ratio, whereas Pool 2 has a low production rate and very low product ratio (i.e., larger contribution of  $N_2O$  reduction). Therefore, in the modelling we assumed individual  $\eta$  values for each pool that can be simulated independently. However, such an approach results in multiple possible results. Hence, we need to begin with assumed values for some of the unknown factors. As the  $\eta_{N_2-N_2O}$  values are lower and less variable than the  $\eta_{N_2O-NO_3}$  values, we first assumed stable (common for both pools)  $\eta_{N_2-N_2O}$  values of  $-6$ ,  $-8$ , and  $-14$ ‰ for  $^{15}N$ ,  $\eta_{SP}$ , and  $^{18}O$ , respectively.<sup>[13]</sup> After setting these values, independent  $\eta_{N_2O-NO_3}$  values for Pools 1 and 2 were found by iteration to reach the best fit between modelled and measured values.

### Determination of $\eta_{N_2-N_2O}$ – Step 3

To fit  $\eta$  values for  $N_2O$  reduction, we assumed stable, common for both pools,  $\eta$  values for  $N_2O$  production, based on the results obtained in Step 2. The average values of all simulated factors for Pool 1 were used. The  $\eta$  values for reduction, independent for Pools 1 and 2, were then found by iteration to reach the best fit between modelled and measured values.

### Coupled determination of $\eta_{N_2O-NO_3}$ and $\eta_{N_2-N_2O}$ – Step 4

The final modelling approach applied the simulation where both unknown factors,  $\eta_{N_2O-NO_3}$  and  $\eta_{N_2-N_2O}$ , individual for each pool, were computed simultaneously. As starting values for iterations, the  $\eta_{N_2-N_2O}$  from Step 2 and the  $\eta_{N_2O-NO_3}$  from Step 3 were used. The introduction of these values – which are already quite well fitted to the dataset and close to the best solution – minimized the uncertainty of the obtained results. These values were then further iterated to reach the best fit between modelled and measured values.

## RESULTS

All three (Step 2, Step 3 and Step 4) modelling strategies were quite successful in predicting the general trend of the observed variations. An example of a selected incubation vessel is shown in Fig. 2, and the data for all the analyzed vessels are presented in the Appendices 2, 3 and 4 (Supporting Information). The Step 4 modelling strategy showed the best compatibility with the measured values for all three values:  $\delta^{15}N$ , SP, and  $\delta^{18}O$  (see Appendix 5,

Supporting Information). It should also be noted that the Step 2 and Step 3 modelling strategies were similarly efficient in predicting the  $\delta^{15}N$  value (Fig. 2(a); Appendix 5, Supporting Information), whereas, for predicting the SP and  $\delta^{18}O$  values, Step 3 modelling worked significantly better than Step 2 (Figs. 2(b) and 2(c); Appendix 5, Supporting Information). Here we present the results of simulated fractionation factors for our three modelling strategies.

### Determined $\eta_{N_2O-NO_3}$ – Step 2

The determined  $\eta^{15}N_{N_2O-NO_3}$  values showed wide variations for all treatments and both pools, from  $-47.1$  to  $-22.1\%$ , and indicated a significantly ( $P < 0.001$ ) smaller NIE for Pool 1 with a mean value of  $-26\%$  than for Pool 2 with a mean value of  $-41\%$ . The  $\eta_{SP_{N_2O-NO_3}}$  values for all treatments for Pool 1 ranged from  $-4.3$  to  $-1.4\%$  with a mean value of  $-3.0\%$ , whereas for Pool 2 all values were below  $-10.6\%$ . Similarly, the  $\eta^{18}O_{N_2O-H_2O}$  values were negative for Pool 2, with a mean of  $-11.5\%$ , whereas the Pool 1 values ranged from  $38.2$  to  $42.1\%$  with a mean value of  $40.8\%$  (Table 1).

### Determined $\eta_{N_2-N_2O}$ – Step 3

The determined  $\eta^{15}N_{N_2-N_2O}$  values for all treatments and both pools varied between  $-8.6$  and  $-0.5\%$  with a mean value of  $-4.3\%$ , the  $\eta_{SP_{N_2-N_2O}}$  values ranged from  $-8.2$  to  $-0.9\%$  with a mean value of  $-4.4\%$ , and the  $\eta^{18}O_{N_2-N_2O}$  values varied between  $-12.4$  and  $+1.1\%$  with a mean value of  $-5.7\%$  (Table 1). The  $\eta$  values for all three isotopic signatures indicated a significantly ( $P < 0.001$ ) smaller NIE for Pool 2 than for Pool 1.

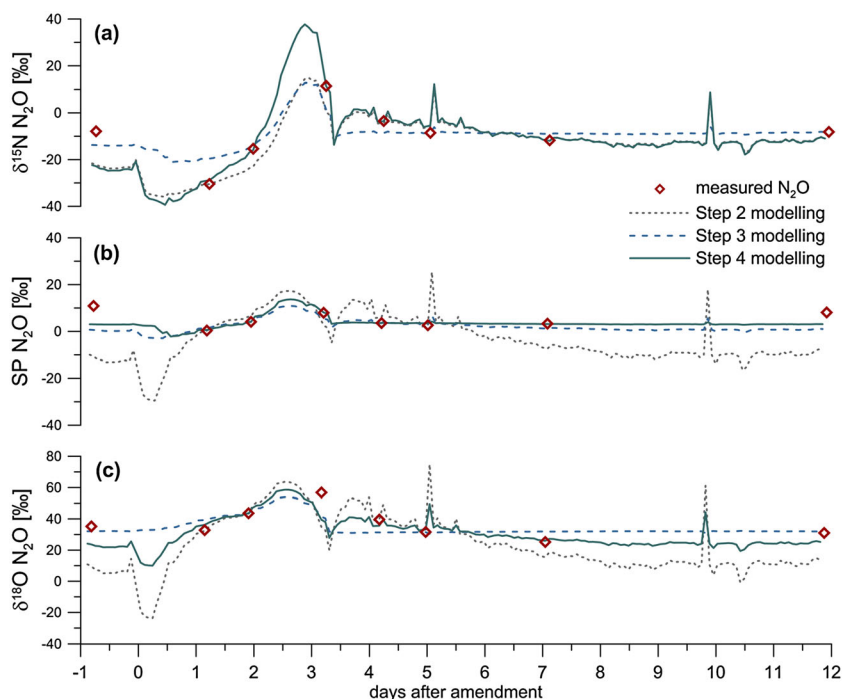


**Figure 2.** Comparison of modelled and measured data for three modelling steps for  $\delta^{15}N$  (a), SP (b), and  $\delta^{18}O$  (c) values for one selected incubation vessel (V2).

**Table 1.** Modelled  $\eta$  values for  $N_2O$  production ( $\eta_{N_2O-NO_3}$ ) and  $N_2O$  reduction ( $\eta_{N_2-N_2O}$ ) according to the presented modelling strategies (Step 2, Step 3, Step 4). The mean values (with standard deviation) for three vessels in each treatment are shown

Modelling	Treatment	$^{15}N$						$^{18}O$					
		$\eta_{N_2O-NO_3}$		$\eta_{N_2-N_2O}$		$\eta_{N_2O-NO_3}$		$\eta_{N_2-N_2O}$		$\eta_{N_2O-H_2O}$		$\eta_{N_2-N_2O}$	
		Pool 1	Pool 2	Pool 1	Pool 2	Pool 1	Pool 2	Pool 1	Pool 2	Pool 1	Pool 2	Pool 1	Pool 2
Step 2	SAT	-22.1 (0.4)	-40.9 (5.6)	-5.7	-2.2 (0.3)	-3.3 (2.6)	-30.9 (9.6)	-8.0	-1.6 (0.4)	42.0 (6.7)	-12.2 (14.4)	-12.2 (4.8)	-1.7 (0.3)
	HALFSAT	-31.3 (4.5)	-47.1 (4.9)	-5.7 (1.2)	-1.6 (1.1)	-1.4 (1.0)	-39.2 (9.8)	-6.6 (0.9)	-0.9 (1.1)	42.1 (2.1)	-12.5 (9.0)	-8.6 (0.2)	-0.3 (0.8)
	UNSAT	-25.9 (7.3)	-36.1 (5.6)	-6.9 (6.8)	-0.5 (0.2)	-4.3 (4.3)	-10.6 (9.8)	-8.2 (5.7)	-3.0 (1.0)	38.2 (3.1)	-9.9 (16.2)	-12.4 (5.1)	1.1 (1.9)
Step 3	SAT	-26.0	-26.0	-8.6 (1.1)	-2.2 (0.3)	-3.0	-3.0	-6.6 (1.5)	-1.6 (0.4)	40.8	40.8	-12.2 (4.8)	-1.7 (0.3)
	HALFSAT			-5.7 (1.2)	-1.6 (1.1)			-6.6 (0.9)	-0.9 (1.1)			-8.6 (0.2)	-0.3 (0.8)
	UNSAT			-6.9 (6.8)	-0.5 (0.2)			-8.2 (5.7)	-3.0 (1.0)			-12.4 (5.1)	1.1 (1.9)
Step 4	SAT	-26.4 (1.5)	-34.0 (6.1)	-8.7 (1.8)	-4.0 (1.8)	0.1 (2.5)	-5.6 (7.2)	-4.6 (2.4)	-2.2 (1.9)	43.3 (1.9)	25.1 (5.5)	-10.6 (4.2)	-5.0 (1.2)
	HALFSAT	-33.5 (8.2)	-44.7 (4.3)	-9.1 (5.8)	-5.3 (0.9)	-1.8 (4.9)	-5.6 (6.8)	-6.0 (2.2)	-1.3 (1.3)	39.2 (2.2)	24.5 (10.4)	-9.3 (1.8)	-3.6 (1.9)
	UNSAT	-25.4 (4.8)	-32.4 (6.2)	-7.3 (2.9)	-2.5 (2.1)	-0.5 (2.0)	3.8 (5.8)	-5.7 (2.4)	-0.2 (1.8)	36.6 (3.8)	30.8 (3.0)	-16.0 (4.8)	-2.5 (0.5)

### Co-determined $\eta_{N_2O-NO_3}$ and $\eta_{N_2-N_2O}$ – Step 4

All the trends observed in the previous modelling steps were also found here. Namely, for  $\eta^{15}N_{N_2O-NO_3}$  significantly ( $P < 0.01$ ) less negative values were obtained for each vessel for Pool 1 than for Pool 2. Conversely, for  $\eta^{15}N_{N_2-N_2O}$ , significantly ( $P < 0.001$ ) smaller NIE were always observed for Pool 2. Exactly the same patterns were noted for  $\eta^{18}O_{N_2-N_2O}$  and  $\eta^{18}O_{N_2O-NO_3}$  ( $P < 0.001$ ). The  $\eta^{18}O_{N_2O-NO_3}$  values ranged from -5.6 to +3.8 (Table 1), with no statistically significant difference between Pool 1 and Pool 2. For the  $\eta^{18}O_{N_2O-H_2O}$  values significantly ( $P < 0.001$ ) higher values were obtained for Pool 1, but the difference between pools was less pronounced with decreasing soil moisture.

The results from this final Step 4 modelling gave the best fit between measured and modelled data (as shown in the comparison presented in Appendix 5, Supporting Information) and provided  $\eta$  values for production and reduction simultaneously. Therefore, these results were accepted as the closest to reality and will be further analyzed and discussed.

### Sensitivity tests

The reliability of the modelled  $\eta$  values is dependent on the accuracy of the input parameters for the model. Hence, we have analyzed various scenarios, where the crucial input parameters were changed to determine the uncertainty of the final results. In those various scenarios the maximum possible error in the gas flux measurements, isotopic analyses of  $N_2O$  and assessment of isotopic signature of source nitrate were taken into account (Table 2).  $N_2$  and the  $N_2O$  fluxes were varied independently in the range of  $\pm 10\%$  of the measured flux. The analytical uncertainty of the isotopic analyses ( $1\sigma$ ) was 0.2‰, 0.2‰, and 0.8‰ for the  $\delta^{15}N$ ,  $\delta^{18}O$ , and SP values, respectively. Here we assumed the maximum possible error of  $2.5\sigma$ , i.e., 0.5‰, 0.5‰ and 2‰, respectively. In addition, significant uncertainty is also associated with the  $\delta^{15}N$  value for the initial nitrate, which was not determined but adopted from the literature data. However, the isotopic signatures of fertilizers and soil nitrate from mineralization are surprisingly stable and vary only in the range of  $\pm 2\%$ .<sup>[40]</sup> This uncertainty influences the  $\eta^{15}N$  determination only and was included in our sensitivity analysis (Table 2). An additional source of inaccuracy can be the applied initial values for iterations. To examine this we changed these initial values in the range of  $\pm 5\%$ . We obtained some pronounced differences in  $\eta_{N_2O-NO_3}$  of 3.6‰, 5.3‰ and 8.7‰ for  $\eta^{15}N$ ,  $\eta^{18}O$  and  $\eta^{18}O$ , respectively. Lower discrepancies were noted for  $\eta_{N_2-N_2O}$ , i.e., 0.7‰, 1.7‰ and 3.3‰, respectively. However, these relatively large possible errors associated with the assumed initial values were minimized in our approach by applying the stepwise modelling, which allowed for better assumption of the proper initial values for the final model (Step 4).

### Controlling factors for $\eta_{N_2O-NO_3}$

The correlations between the  $\eta_{N_2O-NO_3}$  values and the measured fluxes of denitrification products and soil moisture were examined (Table 3). We found significant correlations (Table 3) for  $\eta^{15}N$  and  $\eta^{18}O$  with the emission rate of the denitrification products ( $N_2 + N_2O$  flux). However, no relationship was observed between the  $\eta^{18}O$  and the

**Table 2.** Changes in the determined  $\eta$  values due to changes in model input parameters

change in $\eta$ [‰]		Assumed error	Change in $\eta_{\text{N}_2\text{O}-\text{NO}_3}$ [‰]		Change in $\eta_{\text{N}_2-\text{N}_2\text{O}}$ [‰]	
			Mean	Max	Mean	Max
$\eta^{15}\text{N}$	$\delta_{\text{NO}_3^-}$	$\pm 2\%$	1.2	2.7	0.8	1.7
	$\delta_{\text{N}_2\text{O}}$ measured	$\pm 0.5\%$	0.5	1.3	0.1	0.1
$\eta\text{SP}$	$\text{N}_2$ and $\text{N}_2\text{O}$ fluxes	$\pm 10\%$	1.2	4.4	0.6	1.3
	$\delta_{\text{N}_2\text{O}}$ measured	$\pm 2\%$	1.8	2.3	0.2	0.4
$\eta^{18}\text{O}$	$\text{N}_2$ and $\text{N}_2\text{O}$ fluxes	$\pm 10\%$	0.4	2.1	0.5	1.7
	$\delta_{\text{N}_2\text{O}}$ measured	$\pm 0.5\%$	0.9	2.0	0.2	0.3
	$\text{N}_2$ and $\text{N}_2\text{O}$ fluxes	$\pm 10\%$	0.8	2.3	0.4	1.4

production rate. We did not observe any statistically significant correlation between the NIE and soil moisture (Table 3).

### Controlling factors for $\eta_{\text{N}_2-\text{N}_2\text{O}}$

The correlation coefficients between the  $\eta_{\text{N}_2-\text{N}_2\text{O}}$  values and the fluxes of  $\text{N}_2\text{O}$  and  $\text{N}_2$ , product ratio, reduction rate constant ( $K$ ) and soil moisture were examined (Table 3). The reduction rate constant was calculated based on the measured gas fluxes ( $[\text{N}_2\text{O}]$ ,  $[\text{N}_2 + \text{N}_2\text{O}]$ ) for each time step ( $t$ ), as follows:<sup>[10,13]</sup>

$$K = -\frac{\ln[\text{N}_2\text{O}] - \ln[\text{N}_2 + \text{N}_2\text{O}]}{t} \quad (6)$$

The calculated  $K$  values varied between 0 and  $94 \times 10^{-6} \text{ s}^{-1}$  (data not shown). All three  $\eta$  values are significantly correlated with  $\text{N}_2 + \text{N}_2\text{O}$  fluxes. These significant negative correlations (Table 3) mean that the NIE are larger (more negative  $\eta$  values) with larger substrate availability (higher  $\text{N}_2 + \text{N}_2\text{O}$  flux). Moreover, for  $\eta\text{SP}$  and  $\eta^{18}\text{O}$  we found positive correlations with the reduction rate constant ( $K$ ) and inverse correlations with the product ratio (Table 3). This indicates that the NIE are larger (more negative  $\eta$  values) for slower reduction rates (represented in lower  $K$  values and higher product ratios). However, we found less clear correlations for  $\eta^{15}\text{N}$ , existing only for saturated treatments but with low statistical significance (Table 3). No correlation with soil moisture (WFPS) was observed (Table 3).

## DISCUSSION

### $\text{N}_2\text{O}$ production: $\eta_{\text{N}_2\text{O}-\text{NO}_3}$

There are relatively few studies which have determined the NIE associated with denitrification  $\text{N}_2\text{O}$  production using the whole soil microbial community.<sup>[11,14,24,26,39,43]</sup> All the available results are compared in Table 4 with the results from the present study. The previous studies mostly used addition of  $\text{C}_2\text{H}_2$  to inhibit  $\text{N}_2\text{O}$  reduction.<sup>[11,14,26]</sup> Although we used a very different strategy for the determination of isotope effects, the ranges of our obtained values generally fit within the overall range of the other studies for  $\eta^{18}\text{O}$  and  $\eta^{15}\text{N}$  (Table 4). Our values for  $\eta\text{SP}$  were often lower than previously reported in studies of the whole soil microbial

community (Table 4), but were still mostly in the range reported for bacterial pure culture studies, from  $-10$  to  $+2\%$  (Fig. 3).<sup>[16,21,48]</sup> The  $\eta\text{SP}$  values observed in our experiment suggest a dominant contribution of bacterial denitrifiers in our incubated soils. We also cannot exclude significant contribution of nitrifier denitrification which is characterized by a similar range of  $\eta\text{SP}$  values.<sup>[16]</sup>

The range for  $\eta_{\text{N}_2\text{O}-\text{NO}_3}$  values reported in the literature, and in our experiments, is very large. In Fig. 3 a clear distinction between the  $\eta^{18}\text{O}$  and  $\eta^{15}\text{N}$  values for Pools 1 and 2 can be noticed, with significantly lower values for Pool 2. Pool 2 represents the soil volume not reached by the amendment solution and is characterized by a low production rate, in contrast to Pool 1, which represents the soil volume amended by additional C and N input and characterized by enhanced production rates. This shows that the production rate might have a crucial impact on the fractionation factors for N and O isotopes, but not for SP, where similar values were noted for both pools (Fig. 3). Indeed, our factor analysis (Table 4) shows a significant positive correlation with the denitrification rate for  $\eta^{18}\text{O}$  and  $\eta^{15}\text{N}$  but not for SP. This positive correlation means that with increasing process rates less negative  $\eta$  values were obtained, which is consistent with previous studies reporting decreasing NIE for  $^{15}\text{N}$  for higher process rates.<sup>[18,39]</sup> That no relationship was observed between  $\eta\text{SP}$  and the production rate confirms the previous assumption.<sup>[26]</sup>

Recently, the equation of Farquhar *et al.*,<sup>[49]</sup> commonly applied for  $\text{CO}_2$  assimilation, was proposed by Ostrom and Ostrom<sup>[32]</sup> to explain the wide range of NIE observed during denitrification  $\text{N}_2\text{O}$  production. This wide range is probably the result of at least two fractionation steps, i.e., diffusion and enzymatic reaction,<sup>[32]</sup> as described by Farquhar *et al.*:<sup>[49]</sup>

$$\eta_{\text{P-S}} = \varepsilon_a + (\varepsilon_b - \varepsilon_a) \frac{K_1}{K_2 + K_3} \quad (7)$$

When applied to denitrification  $\text{N}_2\text{O}$  production, the constants in Eqn. (7) are: isotopic fractionation factors for diffusion of nitrate into the denitrifying microsite ( $\varepsilon_a$ ), and enzymatic reduction of nitrate to  $\text{N}_2\text{O}$  ( $\varepsilon_b$ ), and rate constants for diffusion into the denitrifying microsite ( $K_1$ ), out of the denitrifying microsite ( $K_2$ ), and for enzymatic reduction ( $K_3$ ).

Our  $\eta^{15}\text{N}$  results are quite consistent with Eqn. (7). Namely, we observe smaller NIE for fast rate reactions typical for Pool 1, where  $K_3$  is increased due to glucose amendment and  $K_1$  is relatively low due to fast exhaustion of nitrate for enzymatic

**Table 3.** Pearson's correlation coefficients (*r*) between N<sub>2</sub>O production ( $\eta_{\text{N}_2\text{O}-\text{NO}_3}$ ) or N<sub>2</sub>O reduction ( $\eta_{\text{N}_2\text{O}-\text{N}_2\text{O}}$ ) isotope effects and denitrification fluxes (N<sub>2</sub> + N<sub>2</sub>O), product ratio (N<sub>2</sub>O/(N<sub>2</sub> + N<sub>2</sub>O)), reduction rate constant (*K*) and soil moisture (in % WFPS). The *r* values are given for all samples (*n* = 18) as well as separately for SAT (S), HALFSAT (H) and UNSAT (U) treatments (*n* = 6). Statistically significant correlations for  $\alpha = 0.05$  are marked with bold font

	Data set	(N <sub>2</sub> + N <sub>2</sub> O) flux	N <sub>2</sub> flux	N <sub>2</sub> O/(N <sub>2</sub> + N <sub>2</sub> O)	K	WFPS
production $\eta_{\text{N}_2\text{O}-\text{NO}_3}$	All	<b>0.52</b>				-0.14
	S/H/U	0.75/0.71/0.44				
	All	0.22				-0.36
reduction $\eta_{\text{N}_2-\text{N}_2\text{O}}$	All	<b>0.68</b>				0.01
	S/H/U	0.87/0.76/0.62				
	All	<b>-0.59</b>	<b>-0.54</b>	-0.31	0.39	-0.20
	S/H/U	-0.86/-0.59/-0.66	-0.83/-0.63/-0.32	-0.80/-0.53/-0.50	0.84/0.54/0.37	
	All	<b>-0.59</b>	-0.34	<b>-0.68</b>	<b>0.67</b>	-0.08
	All	<b>-0.21</b>	<b>-0.14</b>	<b>-0.76</b>	<b>0.82</b>	<b>0.13</b>
	S/H/U	-0.85/-0.71	-0.87/-0.17	-0.78/-0.92	0.70/0.83	
	All	<b>-0.84</b>	<b>-0.60</b>	<b>-0.68</b>	<b>0.62</b>	
	S/H/U	<b>-0.93</b>	<b>-0.90</b>	<b>-0.58</b>	<b>0.60</b>	<b>0.67</b>

reduction. Hence, the expression  $K_1/(K_2 + K_3)$  approaches 0 and  $\eta$  approaches the fractionation associated with diffusion ( $\epsilon_a$ ), which is significantly lower than fractionation associated with enzymatic reduction.<sup>[26,50]</sup> This would explain the less negative  $\eta^{15}\text{N}$  values obtained for Pool 1.

For  $\eta^{18}\text{O}$  the fractionation mechanism is very different, because of O-exchange with soil water in the course of N<sub>2</sub>O production reaching up to 99%.<sup>[24]</sup> Since the O atom in the produced N<sub>2</sub>O originates mainly from water, its  $\delta^{18}\text{O}$  value depends mainly on the  $\delta^{18}\text{O}$  value of the ambient water and the isotopic fractionation between water and N<sub>2</sub>O. Therefore, the O-isotope effect can be best described by  $\eta^{18}\text{O}_{\text{N}_2\text{O}-\text{H}_2\text{O}}$  values. In previous studies these values were not given, so for our comparison (Table 4) they were calculated using the  $\delta^{18}\text{O}$  values of the produced N<sub>2</sub>O and soil water. In cases of missing data on the  $\delta^{18}\text{O}$  value of soil water, the values from the GNIP (Global Network for Isotopes in Precipitation) database<sup>[44]</sup> were used. The O-exchange between denitrification intermediates and ambient water in the course of nitrate reduction is presumably due to abiotic isotopic equilibrium exchange.<sup>[22]</sup> Therefore, the exchange should show more the characteristic of equilibrium fractionation than a kinetic one and, in consequence, the apparent isotope effect ( $\eta^{18}\text{O}_{\text{N}_2\text{O}-\text{H}_2\text{O}}$ ) should be stable, when near complete O-exchange is assumed. However, we do notice large variations in these values (Table 4). The lowest observed  $\eta^{18}\text{O}_{\text{N}_2\text{O}-\text{H}_2\text{O}}$  values of about +20‰ are not far from the isotope effect associated with abiotic exchange of +14‰ determined by Casciotti *et al.*<sup>[51]</sup> Very similar  $\eta^{18}\text{O}_{\text{N}_2\text{O}-\text{H}_2\text{O}}$  values, of around +19‰, were also reported recently for experiments where almost complete (99%) O-exchange with soil water was documented.<sup>[24]</sup> Similar values are observed in the present study for slow rate production (Pool 2, Fig. 3), but for fast rate production significantly higher  $\eta^{18}\text{O}_{\text{N}_2\text{O}-\text{H}_2\text{O}}$  values of up to +46‰ were found. This large difference may be due to a variable contribution of O-exchange with soil water depending on production rates. It could be assumed that the higher values are due to a lower magnitude of O-exchange<sup>[24]</sup> when the production rates are high. The observed significant correlation between  $\eta^{18}\text{O}_{\text{N}_2\text{O}-\text{H}_2\text{O}}$  and denitrification flux (Table 3) thus suggests that the ratio of exchanged O isotopes can be a function of production rate. This effect may be associated with nitrite concentration in the denitrifying cells, as suggested by Rohe *et al.*,<sup>[52]</sup> since the majority of O-exchange probably occurs during nitrite reduction<sup>[17]</sup> and increases with lower nitrite concentrations.<sup>[52]</sup> The relationship between O-exchange and N<sub>2</sub>O production rate has rarely been discussed, but, from reported experimental results, it seems that the  $\delta^{18}\text{O}_{\text{N}_2\text{O}}$  value increases with increasing N<sub>2</sub>O flux.<sup>[11,26,35,44]</sup> On the other hand, Snider *et al.*,<sup>[43]</sup> based on a <sup>18</sup>O-tracer experiment, reported that the rate of N<sub>2</sub>O production did not influence the magnitude of the O-exchange. However, the results from their natural abundance experiment<sup>[43]</sup> showed that for a low production rate, a lower  $\eta^{18}\text{O}_{\text{N}_2\text{O}-\text{H}_2\text{O}}$  value (about 25‰) was observed than for a high production rate (about 45‰). If we assume that the magnitude of O-exchange is stable, as shown by the <sup>18</sup>O-tracer experiment,<sup>[43]</sup> the relationship between  $\eta^{18}\text{O}_{\text{N}_2\text{O}-\text{H}_2\text{O}}$  and the production rate might be due to an isotopic fractionation mechanism, similar to the one observed for <sup>15</sup>N, dependent on process rate. In summary, from our results it is clear that  $\eta^{18}\text{O}_{\text{N}_2\text{O}-\text{H}_2\text{O}}$  depends on the process rate



**Table 4.** Comparison of reported NIE [in ‰] associated with N<sub>2</sub>O production and reduction during denitrification

N <sub>2</sub> O production				N <sub>2</sub> O reduction								Reference		
$\eta^{15}\text{N}_{\text{N}_2\text{O}-\text{NO}_3}$	$\eta^{\text{SP}}_{\text{N}_2\text{O}-\text{NO}_3}$	$\eta^{18}\text{O}_{\text{N}_2\text{O}-\text{H}_2\text{O}}$	$\eta^{15}\text{N}_{\text{N}_2-\text{N}_2\text{O}}$	$\eta^{\text{SP}}_{\text{N}_2-\text{N}_2\text{O}}$	$\eta^{18}\text{O}_{\text{N}_2-\text{N}_2\text{O}}$ [‰]	$\eta^{18}\text{O}/\eta^{15}\text{N}$	$\eta^{18}\text{O}/\eta^{\text{SP}}$							
min	max	min	max	min	max	min	max	min	max	min	max	min	max	
-27	-32	+12	+20	-9.8	-6.3	-24.9	-12.6	1.6	2.7	1.6	2.7	1.6	2.7	Mariotti <i>et al.</i> <sup>[39]</sup>
-29	-24	+28	+57	-9.2	-1.8	-25.1	-5.1	2.3	2.7	2.3	2.7	2.3	2.7	Menyailo and Hungate <sup>[11]</sup>
-45	-10	+17		-36.0	-1.0	-74.0	-6.9	2.1	2.7	2.1	2.7	2.1	2.7	Perez <i>et al.</i> <sup>[14]</sup>
				-7.8	-4.2	-19.1	-12.5	1.9	2.6	1.9	2.6	1.9	2.6	Ostrom <i>et al.</i> <sup>[12]</sup>
				-8.8	-5.1	-19.8	-11.4	2.2	2.4	2.2	2.4	2.2	2.4	Vieten <i>et al.</i> <sup>[27]</sup>
				-11.0	-4.6	-18.4	-15.7	1.6	3.8	1.6	3.8	1.6	3.8	Jinuntuya-
				-5.8	+16.2	-9.4	+8.9	-0.3	5.1	-0.3	5.1	-0.3	5.1	Nortman <i>et al.</i> <sup>[10]</sup>
				-9.1	-2.5	-16.0	-2.5	0.7	2.2	0.7	2.2	0.7	2.2	Nortman <i>et al.</i> <sup>[10]</sup>
				-8.8	-5.1	-19.8	-11.4	2.2	2.4	2.2	2.4	2.2	2.4	Well and Flessa <sup>[13]</sup>
				-11.0	-4.6	-18.4	-15.7	1.6	3.8	1.6	3.8	1.6	3.8	Well and Flessa <sup>[26]</sup>
				-5.8	+16.2	-9.4	+8.9	-0.3	5.1	-0.3	5.1	-0.3	5.1	Snider <i>et al.</i> <sup>[43]</sup>
				-9.1	-2.5	-16.0	-2.5	0.7	2.2	0.7	2.2	0.7	2.2	static <sup>c</sup> , Lewicka-
				-8.8	-5.1	-19.8	-11.4	2.2	2.4	2.2	2.4	2.2	2.4	Szczebak <i>et al.</i> <sup>[24]</sup>
				-11.0	-4.6	-18.4	-15.7	1.6	3.8	1.6	3.8	1.6	3.8	dynamic <sup>b</sup> , Lewicka-
				-5.8	+16.2	-9.4	+8.9	-0.3	5.1	-0.3	5.1	-0.3	5.1	Szczebak <i>et al.</i> <sup>[24]</sup>
				-9.1	-2.5	-16.0	-2.5	0.7	2.2	0.7	2.2	0.7	2.2	Szczebak <i>et al.</i> <sup>[24]</sup>
				-8.8	-5.1	-19.8	-11.4	2.2	2.4	2.2	2.4	2.2	2.4	<i>present study</i> <sup>c</sup>

<sup>a</sup>Experiment 1: static incubations: closed incubation vessels, N<sub>2</sub>O accumulated, Lewicka-Szczebak *et al.*<sup>[24]</sup>

<sup>b</sup>Experiments 2 and 3: dynamic incubations in a flow-through system, Lewicka-Szczebak *et al.*<sup>[24]</sup>

<sup>c</sup>Reported values for *the present study* are the summarized mean values of each water saturation treatment (as presented in Table 1 with respective standard deviations).

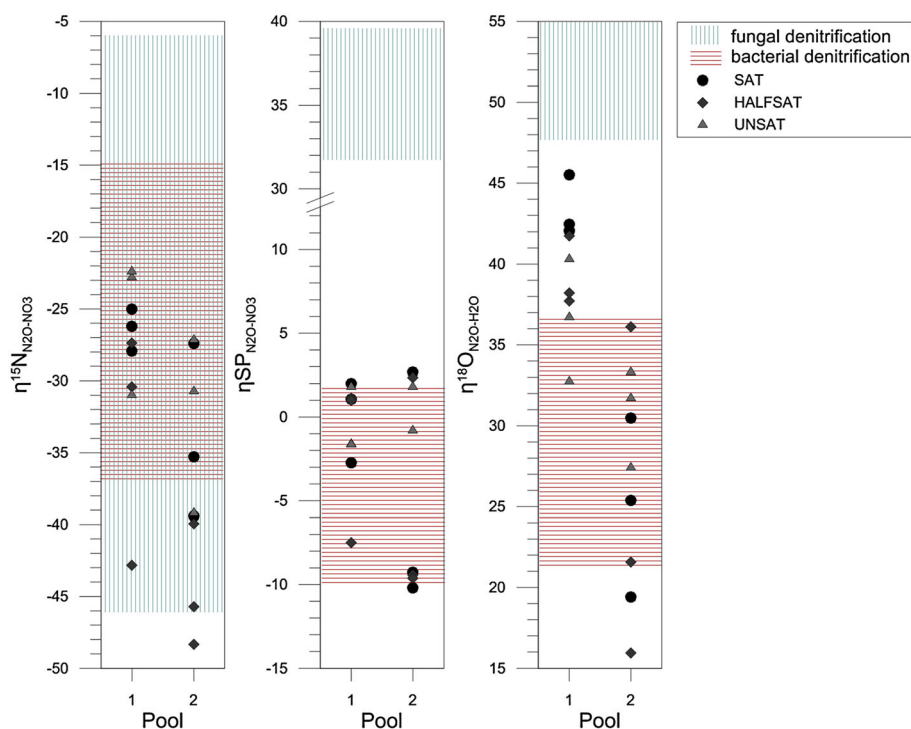


**Figure 3.** The calculated isotopic fractionation factors ( $\eta$ ) associated with  $\text{N}_2\text{O}$  production during denitrification emitted by different soil pools (1 and 2, X axis) and by various water treatments (various symbols). The range defined by previous pure culture studies for denitrification is indicated by the striped fields separately for bacterial and fungal denitrifiers, based on the summary presented by Toyoda *et al.*<sup>[30]</sup>  $\eta^{18}\text{O}_{\text{N}_2\text{O}-\text{H}_2\text{O}}$  was calculated from the results presented by Toyoda *et al.*<sup>[21]</sup> Sutka *et al.*<sup>[18]</sup> and Rohe *et al.*<sup>[17]</sup> The values for fungal denitrification represent the incubations with both  $\text{NO}_2^-$  and  $\text{NO}_3^-$  as electron acceptor.<sup>[17,18]</sup>

(Table 3), which can be due either to the varying magnitude of O-exchange or to varying isotopic fractionation between soil water and the produced  $\text{N}_2\text{O}$  in relation to the process rate. Further studies are needed to clarify this.

#### $\text{N}_2\text{O}$ reduction: $\eta_{\text{N}_2-\text{N}_2\text{O}}$

There are a few studies which have determined the NIE associated with denitrification  $\text{N}_2\text{O}$  reduction using the whole soil microbial community.<sup>[10–13,24,27]</sup> All the available data are compared with results from the present study in Table 4.

The range of values obtained in the present study is mostly within the range of previous experiments, but the ratios of  $\eta^{18}\text{O}/\eta^{15}\text{N}$  and  $\eta^{18}\text{O}/\eta^{\text{SP}}$  differ quite significantly from the majority of previous data (Table 4). In almost all previous reduction experiments, quite stable and consistent  $\eta^{18}\text{O}/\eta^{15}\text{N}$  ratios of about 2.5 were obtained (Table 4). Since this ratio was quite stable, it has been proposed as a tool to estimate the contribution of reduced  $\text{N}_2\text{O}$ .<sup>[11,13]</sup> In some recent studies authors used this ratio to prove the absence of  $\text{N}_2\text{O}$  reduction, based on the fact that they observed a slope for  $\delta^{18}\text{O}/\delta^{15}\text{N}$  of less than 1.<sup>[28,53]</sup> However, in the majority of our results the  $\eta^{18}\text{O}/\eta^{15}\text{N}$  ratio was below 2, and occasionally below 1, especially for a low product ratio. Could the stable  $\eta^{18}\text{O}/\eta^{15}\text{N}$  ratio obtained in previous studies be an artefact of the experimental set-up? All these former  $\text{N}_2\text{O}$  reduction experiments were based on the

methodology where  $\text{N}_2\text{O}$  was added to the headspace of nitrate-free incubated soil.<sup>[10–13,27]</sup> An alternative indirect method was proposed only very recently,<sup>[24]</sup> based on the comparison of experimental treatments with and without inhibition of  $\text{N}_2\text{O}$  reduction (using the  $\text{C}_2\text{H}_2$  addition method), where significantly higher, partially even positive,  $\eta$  values were obtained. The determined values for NIE were highly dependent on the applied experimental set-up,<sup>[24]</sup> i.e., by static incubations in closed vessels, where  $\text{N}_2\text{O}$  accumulates in the headspace, the obtained  $\eta$  values were similar to those in the previous experiments, whereas, under dynamic conditions with constant flushing of the headspace, the  $\eta^{18}\text{O}$  and  $\eta^{15}\text{N}$  values were less negative (Table 4; Fig. 4). The  $\eta^{\text{SP}}$  was, however, independent of the experimental set-up (Fig. 4).

In nature, there are two coexisting routes for  $\text{N}_2\text{O}$  reduction: (1) within the microsite prior to escape, and (2) upon re-entering the denitrifying microsite.<sup>[12,24]</sup> Only pathway (2) can be monitored when using the  $\text{N}_2\text{O}$  addition method. In this study we applied a method where  $\text{N}_2\text{O}$  production and reduction occur simultaneously; hence, the contribution of these two reduction pathways should most closely reflect the typical natural conditions. Probably the very stable  $\eta^{18}\text{O}/\eta^{15}\text{N}$  ratios obtained previously in the  $\text{N}_2\text{O}$  addition experiments are characteristic for enzymatic fractionation factors for  $^{18}\text{O}$  and  $^{15}\text{N}$ . For diffusive fractionation factors, the  $\eta^{18}\text{O}/\eta^{15}\text{N}$  ratio is lower;<sup>[50]</sup> hence, the lower values of this ratio observed in this experiment suggest

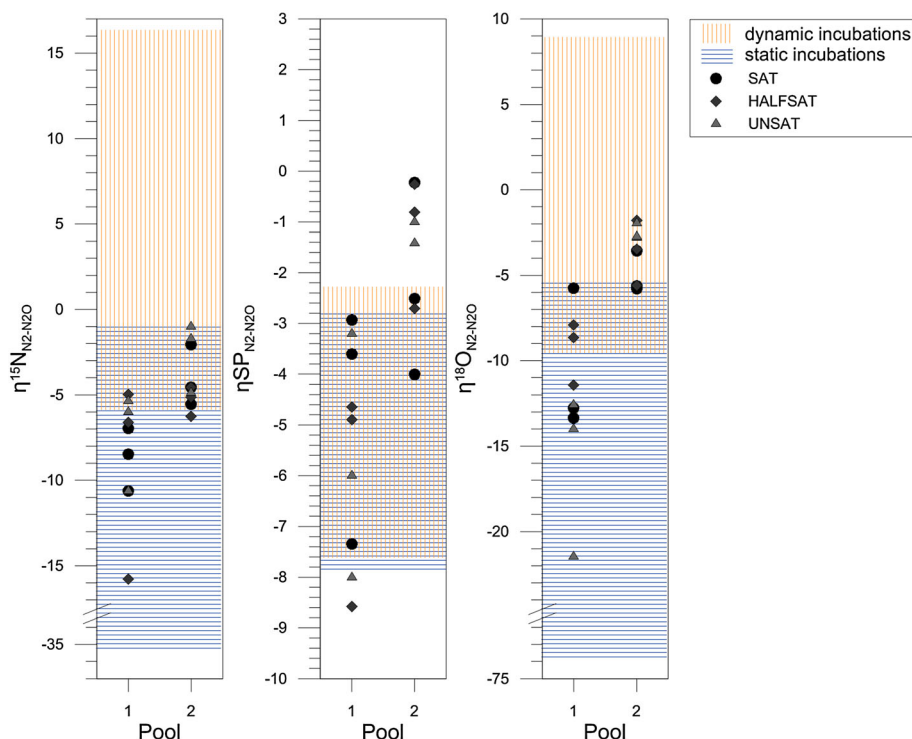


**Figure 4.** The calculated isotopic fractionation factors ( $\eta$ ) associated with  $\text{N}_2\text{O}$  reduction during denitrification emitted by different soil pools (1 and 2, X axis) and by various water treatments (various symbols). The range defined by previous studies (with entire soil microbial community) is indicated by the striped fields separately for static and dynamic conditions (see Table 8 for precise values).

a larger contribution of route (1) reduction, where a high contribution of  $\text{N}_2\text{O}$  diffused from the microsite before reduction. Nevertheless, route (2) must be also active, since we do not observe the inverse NIE, i.e., positive  $\eta$  values, as was the case in our previous experiment where route (1) must have been dominant.<sup>[24]</sup> In this study we deal with very wet conditions which probably favor the accumulation of  $\text{N}_2\text{O}$  in microsites, facilitating its further reduction and preventing its fast escape. This results in a lower fraction of diffused  $\text{N}_2\text{O}$ , and, consequently, in more negative  $\eta$  values, as shown in the model calculations by Lewicka-Szczebak *et al.*<sup>[24]</sup>

Generally, the range of NIE values determined by our experiments for Pool 1 is within that of previous data for static incubations, showing almost exactly the same range for  $\eta_{\text{SP}}$  values, and for  $\eta^{15}\text{N}$  and  $\eta^{18}\text{O}$  the values are close to the highest values of the range determined by the previous static studies.<sup>[10–13,24]</sup> Significantly higher values were found for Pool 2 (Fig. 4). Pool 2 represents the unamended soil volume, which is characterized by a low product ratio, in contrast to Pool 1, which represents the amended soil volume characterized by a higher product ratio. The amendment solution was added on the soil surface; hence, the Pool 1 emission was close to the soil surface, and consequently, the path length of  $\text{N}_2\text{O}$  diffusion was short (0 to few mm), whereas the path length for Pool 2 was much longer, up to 100 mm. This spatial difference probably governs the balance between the significance of the enzymatic and the diffusive fractionation. For Pool 1 the short diffusion path length may result in an insignificant fractionation effect associated with diffusion, and in consequence the observed  $\eta$  values result

mainly from the enzymatic fractionation, and hence are similar to those from the previous  $\text{N}_2\text{O}$  addition experiments. For Pool 2 the effect of diffusive fractionation is larger due to the longer  $\text{N}_2\text{O}$  diffusion path length; hence, we observe smaller NIE, typical for a mixture of diffusive and enzymatic effects, which is consistent with the reduction model proposed by Lewicka-Szczebak *et al.*<sup>[24]</sup>

Moreover, we must consider that the highest  $\eta$  values are noted for Pool 2 (Fig. 4), where we deal with extremely low product ratio, which means that the vast majority of the produced  $\text{N}_2\text{O}$  has been reduced to  $\text{N}_2$ . In such a case it is theoretically possible that in the soil microsites all the  $\text{N}_2\text{O}$  is reduced; hence, there is no residual  $\text{N}_2\text{O}$  and the information on NIE from those microsites is lost. In such a case our model would underestimate the  $\eta$  values, because the measured residual  $\text{N}_2\text{O}$  is insufficiently enriched in heavy isotopes according to the determined reduction progress. This assumption may be supported by the values observed for  $\eta_{\text{SP}}$  for Pool 2, which were much less negative than those observed in all the previous experiments. As was shown recently, the  $\eta_{\text{SP}}$  values are very robust and not influenced by the experimental setup; hence, the less negative values observed here cannot be explained by the balance between different reduction routes,<sup>[24]</sup> but are probably due to complete  $\text{N}_2\text{O}$  reduction in dead-end pores. Therefore, the strategy of simultaneous measurements of isotope effects during  $\text{N}_2\text{O}$  production and reduction is more robust when the product ratio does not reach extremely low values. Therefore, from the results obtained for  $\eta_{\text{N}_2-\text{N}_2\text{O}}$  the values presented for Pool 1 probably provide the best estimates for

the true fractionation factors. When only taking these values into consideration, it can be concluded that the very robust  $\eta_{\text{SP}_{\text{N}_2\text{-N}_2\text{O}}}$  value of ca  $-5\%$  defined previously<sup>[24]</sup> can be confirmed again. However, it should be kept in mind that when we deal with extremely low product ratios, the typical fractionation factors and typical  $\eta^{18}\text{O}/\eta^{15}\text{N}$  ratios are probably not valid.

### Limitations of the calculations applied and future perspectives

The modelling approach presented here was quite challenging because of the complex dynamics of the experimental setup. The existence of two pools adds uncertainty to the provided results, since the division of measured emissions into two pools may not be fully accurate, because the size and dynamics of both pools are not known. Hence, the observed trends should be confirmed by future experiments using a simpler setup where the emissions originate from one homogenous pool only.

For calculations of NIE associated with  $\text{N}_2\text{O}$  reduction, the closed system approach based on Rayleigh equations was accepted according to the previous observations which have been discussed elsewhere and justified this approach.<sup>[23,24]</sup> For this experiment the closed system dynamics should be most appropriate, since all the treatments were extremely wet and such conditions facilitate the accumulation of  $\text{N}_2\text{O}$  in the soil pores. In such cases the  $\text{N}_2\text{O}$  pool undergoes isotopic fractionation according to closed system equations.<sup>[54]</sup> This must clearly be the case for Pool 1, because of high  $\text{N}_2\text{O}$  production. However, in Pool 2, characterized by the very low product ratio, nearly all the produced  $\text{N}_2\text{O}$  is reduced. It is reasonable to assume that in such cases the open system dynamics might be applicable, since there is probably no  $\text{N}_2\text{O}$  reservoir formed in soil pores. If the open system equations were used here, we would obtain more negative  $\eta$  values for Pool 2, hence closer to the results from Pool 1 and previous literature data (Fig. 4). Therefore, the interpretation of the less negative  $\eta_{\text{N}_2\text{-N}_2\text{O}}$  values obtained for Pool 2 is quite ambiguous, since this may be a result of: (i) large contribution of diffusive effects due to  $\text{N}_2\text{O}$  escape through the long diffusion path, (ii) complete  $\text{N}_2\text{O}$  reduction in the dead-end pores which underestimates the actual NIE, or (iii) inappropriate usage of closed system dynamics which also underestimates the actual NIE. To date, we have not been able to prove the relative significance of each of these issues. The examination of fractionation factors for various product ratios and reaction rates should be addressed by future studies to develop a model combining isotopic fractionation with spatial dispersion of production and reduction and with diffusive fluxes allowing the prediction of full  $\text{N}_2\text{O}$  consumption in isolated soil pores.

It should be noted that this experiment was characterized by extremely high denitrification rates up to approx.  $50 \text{ mg N kg}^{-1} \text{ day}^{-1}$  for Pool 1 and approx.  $5 \text{ mg N kg}^{-1} \text{ day}^{-1}$  for Pool 2. Hence, the fractionation factors obtained for these very artificial conditions may not be fully transferable to the natural field studies. Although the observed relationships between NIE and process dynamics is extending our understanding of the isotopic signatures of soil emitted  $\text{N}_2\text{O}$  and its use to constrain  $\text{N}_2\text{O}$  processes, the database of this

study does not cover typical soil conditions. There is a need for further studies applying the conditions more closely to natural field studies.

### SUMMARY

In the present study, the fractionation factors associated with denitrification processes were determined for the first time in a controlled experiment under an oxic atmosphere, where the entire denitrification process occurs within a single incubation vessel. The obtained magnitudes of fractionation factors associated with  $\text{N}_2\text{O}$  production and reduction generally confirmed the range of values reported by previous studies. Our results showed that higher denitrification rates resulted in decreasing net isotope effects during  $\text{N}_2\text{O}$  production for  $^{15}\text{N}$ . Similarly, a clear relationship of  $\eta^{18}\text{O}_{\text{N}_2\text{O-H}_2\text{O}}$  values and process rates was observed, probably due to the varying magnitude of O-exchange with soil water or varying isotopic fractionation associated with this exchange. The SP values of produced  $\text{N}_2\text{O}$  did not show significant variations in relation to soil moisture or to process rates.

For  $\text{N}_2\text{O}$  reduction clearly diverse net isotope effects were observed for the two distinct soil pools. For Pool 1, representing amended soil and showing high fluxes but moderate product ratio, the  $\eta$  values and the characteristic  $\eta^{18}\text{O}/\eta^{15}\text{N}$  ratios were similar to those previously reported. However, for Pool 2, representing the unamended soil characterized by lower fluxes and very low product ratio, the net isotope effects were much smaller and the  $\eta^{18}\text{O}/\eta^{15}\text{N}$  ratios, previously accepted as typical for  $\text{N}_2\text{O}$  reduction processes (i.e., higher than 2), were not valid.

### Acknowledgements

This study was supported by the German Research Foundation (DFG, We/1904-4) and the UK Biotechnology and Biological Sciences Research Council (BBSRC, BBE0015801). We would like to acknowledge Mark Butler for his contribution to the experimental work. Rothamsted Research uses facilities funded by BBSRC.

### REFERENCES

- [1] M. K. Firestone, E. A. Davidson, in *Exchange of Trace Gases Between Terrestrial Ecosystems and the Atmosphere*. (Eds: M. O. Andreae, D. S. Schimel). John Wiley, New York, **1989**, p. 7.
- [2] D. E. Canfield, A. N. Glazer, P. G. Falkowski. The evolution and future of Earth's nitrogen cycle. *Science* **2010**, *330*, 192.
- [3] IPCC, in *Climate Change 2013*, (Eds: T. F. Stocker, D. Qin, G. K. Plattner, M. Tignor, S. K. Allen, J. Boschung, A. Nauels, Y. Xia, V. Bex, P. M. Midgley). Intergovernmental Panel on Climate Change, Cambridge and New York, **2013**, p. 1553.
- [4] A. R. Ravishankara, J. S. Daniel, R. W. Portmann. Nitrous oxide ( $\text{N}_2\text{O}$ ): The dominant ozone-depleting substance emitted in the 21<sup>st</sup> century. *Science* **2009**, *326*, 123.
- [5] O. Mathieu, J. Leveque, C. Henault, M. J. Milloux, F. Bizouard, F. Andreux. Emissions and spatial variability of  $\text{N}_2\text{O}$ ,  $\text{N}_2$  and

- nitrous oxide mole fraction at the field scale, revealed with  $^{15}\text{N}$  isotopic techniques. *Soil Biol. Biochem.* **2006**, *38*, 941.
- [6] J. L. Morse, E. S. Bernhardt. Using  $^{15}\text{N}$  tracers to estimate  $\text{N}_2\text{O}$  and  $\text{N}_2$  emissions from nitrification and denitrification in coastal plain wetlands under contrasting land-uses. *Soil Biol. Biochem.* **2013**, *57*, 635.
  - [7] M. Senbayram, R. Chen, A. Budai, L. Bakken, K. Dittert.  $\text{N}_2\text{O}$  emission and the  $\text{N}_2\text{O}/(\text{N}_2\text{O}+\text{N}_2)$  product ratio of denitrification as controlled by available carbon substrates and nitrate concentrations. *Agr. Ecosyst. Environ.* **2012**, *147*, 4.
  - [8] C. A. M. Brenninkmeijer, T. Röckmann. Mass spectrometry of the intramolecular nitrogen isotope distribution of environmental nitrous oxide using fragment-ion analysis. *Rapid Commun. Mass Spectrom.* **1999**, *13*, 2028.
  - [9] S. Toyoda, N. Yoshida. Determination of nitrogen isotopomers of nitrous oxide on a modified isotope ratio mass spectrometer. *Anal. Chem.* **1999**, *71*, 4711.
  - [10] M. Jinuntuya-Nortman, R. L. Sutka, P. H. Ostrom, H. Gandhi, N. E. Ostrom. Isotopologue fractionation during microbial reduction of  $\text{N}_2\text{O}$  within soil mesocosms as a function of water-filled pore space. *Soil Biol. Biochem.* **2008**, *40*, 2273.
  - [11] O. V. Menyailo, B. A. Hungate. Stable isotope discrimination during soil denitrification: Production and consumption of nitrous oxide. *Global Biogeochem. Cycles* **2006**, *20*, GB3025.
  - [12] N. E. Ostrom, A. Pitt, R. Sutka, P. H. Ostrom, A. S. Grandy, K. M. Huizinga, G. P. Robertson. Isotopologue effects during  $\text{N}_2\text{O}$  reduction in soils and in pure cultures of denitrifiers. *J. Geophys. Res.-Biogeosciences* **2007**, *112*, G02005.
  - [13] R. Well, H. Flessa. Isotopologue enrichment factors of  $\text{N}_2\text{O}$  reduction in soils. *Rapid Commun. Mass Spectrom.* **2009**, *23*, 2996.
  - [14] T. Perez, D. Garcia-Montiel, S. Trumbore, S. Tyler, P. De Camargo, M. Moreira, M. Piccolo, C. Cerri. Nitrous oxide nitrification and denitrification  $^{15}\text{N}$  enrichment factors from Amazon forest soils. *Ecol. Appl.* **2006**, *16*, 2153.
  - [15] R. Well, H. Flessa, L. Xing, X. T. Ju, V. Romheld. Isotopologue ratios of  $\text{N}_2\text{O}$  emitted from microcosms with  $\text{NH}_4^+$  fertilized arable soils under conditions favoring nitrification. *Soil Biol. Biochem.* **2008**, *40*, 2416.
  - [16] R. L. Sutka, N. E. Ostrom, P. H. Ostrom, J. A. Breznak, H. Gandhi, A. J. Pitt, F. Li. Distinguishing nitrous oxide production from nitrification and denitrification on the basis of isotopomer abundances. *Appl. Environ. Microb.* **2006**, *72*, 638.
  - [17] L. Rohe, T.-H. Anderson, G. Braker, H. Flessa, A. Giesemann, D. Lewicka-Szczebak, N. Wrage-Mönning, R. Well. Dual isotope and isotopomer signatures of nitrous oxide from fungal denitrification – a pure culture study. *Rapid Commun. Mass Spectrom.* **2014**, *28*, 1893.
  - [18] R. L. Sutka, G. C. Adams, N. E. Ostrom, P. H. Ostrom. Isotopologue fractionation during  $\text{N}_2\text{O}$  production by fungal denitrification. *Rapid Commun. Mass Spectrom.* **2008**, *22*, 3989.
  - [19] C. C. Barford, J. P. Montoya, M. A. Altabet, R. Mitchell. Steady-state nitrogen isotope effects of  $\text{N}_2$  and  $\text{N}_2\text{O}$  production in *Paracoccus denitrificans*. *Appl. Environ. Microb.* **1999**, *65*, 989.
  - [20] K. L. Casciotti, D. M. Sigman, M. G. Hastings, J. K. Bohlke, A. Hilker. Measurement of the oxygen isotopic composition of nitrate in seawater and freshwater using the denitrifier method. *Anal. Chem.* **2002**, *74*, 4905.
  - [21] S. Toyoda, H. Mutobe, H. Yamagishi, N. Yoshida, Y. Tanji. Fractionation of  $\text{N}_2\text{O}$  isotopomers during production by denitrifier. *Soil Biol. Biochem.* **2005**, *37*, 1535.
  - [22] D. M. Snider, J. J. Venkiteswaran, S. L. Schiff, J. Spoelstra. Deciphering the oxygen isotope composition of nitrous oxide produced by nitrification. *Glob. Change Biol.* **2012**, *18*, 356.
  - [23] J. R. Köster, R. Well, K. Dittert, A. Giesemann, D. Lewicka-Szczebak, K. H. Mühling, A. Herrmann, J. Lammel, M. Senbayram. Soil denitrification potential and its influence on  $\text{N}_2\text{O}$  reduction and  $\text{N}_2\text{O}$  isotopomer ratios. *Rapid Commun. Mass Spectrom.* **2013**, *27*, 2363.
  - [24] D. Lewicka-Szczebak, R. Well, J. R. Köster, R. Fuss, M. Senbayram, K. Dittert, H. Flessa. Experimental determinations of isotopic fractionation factors associated with  $\text{N}_2\text{O}$  production and reduction during denitrification in soils. *Geochim. Cosmochim. Acta* **2014**, *134*, 55.
  - [25] D. Snider, J. J. Venkiteswaran, S. L. Schiff, J. Spoelstra. A new mechanistic model of  $\delta^{18}\text{O}-\text{N}_2\text{O}$  formation by denitrification. *Geochim. Cosmochim. Acta* **2013**, *112*, 102.
  - [26] R. Well, H. Flessa. Isotopologue signatures of  $\text{N}_2\text{O}$  produced by denitrification in soils. *J. Geophys. Res.-Biogeosciences* **2009**, *114*, G02020.
  - [27] B. Vieten, T. Blunier, A. Neftel, C. Alewell, F. Conen. Fractionation factors for stable isotopes of N and O during  $\text{N}_2\text{O}$  reduction in soil depend on reaction rate constant. *Rapid Commun. Mass Spectrom.* **2007**, *21*, 846.
  - [28] M. R. Opdyke, N. E. Ostrom, P. H. Ostrom. Evidence for the predominance of denitrification as a source of  $\text{N}_2\text{O}$  in temperate agricultural soils based on isotopologue measurements. *Global Biogeochem. Cycles* **2009**, *23*, GB4018.
  - [29] S. Park, T. Perez, K. A. Boering, S. E. Trumbore, J. Gil, S. Marquina, S. C. Tyler. Can  $\text{N}_2\text{O}$  stable isotopes and isotopomers be useful tools to characterize sources and microbial pathways of  $\text{N}_2\text{O}$  production and consumption in tropical soils? *Global Biogeochem. Cycles* **2011**, *25*, GB1001.
  - [30] S. Toyoda, M. Yano, S. Nishimura, H. Akiyama, A. Hayakawa, K. Koba, S. Sudo, K. Yagi, A. Makabe, Y. Tobar, N. O. Ogawa, N. Ohkouchi, K. Yamada, N. Yoshida. Characterization and production and consumption processes of  $\text{N}_2\text{O}$  emitted from temperate agricultural soils determined via isotopomer ratio analysis. *Global Biogeochem. Cycles* **2011**, *25*, GB2008.
  - [31] T. Kato, S. Toyoda, N. Yoshida, Y. H. Tang, E. Wada. Isotopomer and isotopologue signatures of  $\text{N}_2\text{O}$  produced in alpine ecosystems on the Qinghai-Tibetan Plateau. *Rapid Commun. Mass Spectrom.* **2013**, *27*, 1517.
  - [32] N. E. Ostrom, P. H. Ostrom, in *Handbook of Environmental Isotope Geochemistry*, (Ed: M. Baskaran). Springer, **2011**, p. 453.
  - [33] A. S. Gregory, N. R. A. Bird, W. R. Whalley, G. P. Matthews, I. M. Young. Deformation and Shrinkage Effects on the Soil Water Release Characteristic. *Soil Sci. Soc. Am. J.* **2010**, *74*, 1104.
  - [34] A. Bergstermann, L. Cardenas, R. Bol, L. Gilliam, K. Goulding, A. Mejjide, D. Scholefield, A. Vallejo, R. Well. Effect of antecedent soil moisture conditions on emissions and isotopologue distribution of  $\text{N}_2\text{O}$  during denitrification. *Soil Biol. Biochem.* **2011**, *43*, 240.
  - [35] L. M. Cardenas, J. M. B. Hawkins, D. Chadwick, D. Scholefield. Biogenic gas emissions from soils measured using a new automated laboratory incubation system. *Soil Biol. Biochem.* **2003**, *35*, 867.
  - [36] T. Röckmann, J. Kaiser, C. A. M. Brenninkmeijer, W. A. Brand. Gas chromatography/isotope-ratio mass spectrometry method for high-precision position-dependent  $^{15}\text{N}$  and  $^{18}\text{O}$  measurements of atmospheric nitrous oxide. *Rapid Commun. Mass Spectrom.* **2003**, *17*, 1897.
  - [37] M. B. Westley, B. N. Popp, T. M. Rust. The calibration of the intramolecular nitrogen isotope distribution in nitrous oxide measured by isotope ratio mass spectrometry. *Rapid Commun. Mass Spectrom.* **2007**, *21*, 391.
  - [38] R. Well, W. Eschenbach, H. Flessa, C. von der Heide, D. Weymann. Are dual isotope and isotopomer ratios of  $\text{N}_2\text{O}$  useful indicators for  $\text{N}_2\text{O}$  turnover during

- denitrification in nitrate-contaminated aquifers? *Geochim. Cosmochim. Acta* **2012**, *90*, 265.
- [39] A. Mariotti, J. C. Germon, P. Hubert, P. Kaiser, R. Letolle, A. Tardieux, P. Tardieux. Experimental determination of nitrogen kinetic isotope fractionation - some principles - illustration for the denitrification and nitrification processes. *Plant Soil* **1981**, *62*, 413.
- [40] L. Rock, B. H. Ellert, B. Mayer. Tracing sources of soil nitrate using the dual isotopic composition of nitrate in 2 M KCl-extracts. *Soil Biol. Biochem.* **2011**, *43*, 2397.
- [41] A. S. Bateman, S. D. Kelly. Fertilizer nitrogen isotope signatures. *Isot. Environ. Health Stud.* **2007**, *43*, 237.
- [42] D. M. Kool, N. Wrage, O. Oenema, D. Harris, J. W. Van Groenigen. The O-18 signature of biogenic nitrous oxide is determined by O exchange with water. *Rapid Commun. Mass Spectrom.* **2009**, *23*, 104.
- [43] D. M. Snider, S. L. Schiff, J. Spoelstra. N-15/N-14 and O-18/O-16 stable isotope ratios of nitrous oxide produced during denitrification in temperate forest soils. *Geochim. Cosmochim. Acta* **2009**, *73*, 877.
- [44] IAEA. Isotope Hydrology Information System. The ISOHIS Database. **2006**. Available: <http://www.iaea.org/water>.
- [45] D. Fylstra, L. Lasdon, J. Watson, A. Waren. Design and use of the Microsoft Excel Solver. *Interfaces* **1998**, *28*, 29.
- [46] S. Walsh, D. Diamond. Nonlinear curve-fitting using Microsoft Excel Solver. *Talanta* **1995**, *42*, 561.
- [47] A. Meijide, L. M. Cardenas, R. Bol, A. Bergstermann, K. Goulding, R. Well, A. Vallejo, D. Scholefield. Dual isotope and isotopomer measurements for the understanding of N<sub>2</sub>O production and consumption during denitrification in an arable soil. *Eur. J. Soil Sci.* **2010**, *61*, 364.
- [48] R. L. Sutka, N. E. Ostrom, P. H. Ostrom, H. Gandhi, J. A. Breznak. Nitrogen isotopomer site preference of N<sub>2</sub>O produced by *Nitrosomonas europaea* and *Methylococcus capsulatus* Bath. *Rapid Commun. Mass Spectrom.* **2003**, *17*, 738.
- [49] G. D. Farquhar, M. H. O'Leary, J. A. Berry. On the relationship between carbon isotope discrimination and the inter-cellular carbon-dioxide concentration in leaves. *Aust. J. Plant Physiol.* **1982**, *9*, 121.
- [50] R. Well, H. Flessa. Isotope fractionation factors of N<sub>2</sub>O diffusion. *Rapid Commun. Mass Spectrom.* **2008**, *22*, 2621.
- [51] K. L. Casciotti, J. K. Bohlke, M. R. McIlvin, S. J. Mroczkowski, J. E. Hannon. Oxygen isotopes in nitrite: Analysis, calibration, and equilibration. *Anal. Chem.* **2007**, *79*, 2427.
- [52] L. Rohe, T. H. Anderson, G. Braker, H. Flessa, A. Giesemann, N. Wrage-Monnig, R. Well. Fungal oxygen exchange between denitrification intermediates and water. *Rapid Commun. Mass Spectrom.* **2014**, *28*, 377.
- [53] N. E. Ostrom, R. Sutka, P. H. Ostrom, A. S. Grandy, K. M. Huizinga, H. Gandhi, J. C. von Fischer, G. P. Robertson. Isotopologue data reveal bacterial denitrification as the primary source of N<sub>2</sub>O during a high flux event following cultivation of a native temperate grassland. *Soil Biol. Biochem.* **2010**, *42*, 499.
- [54] B. Fry. *Stable Isotope Ecology*. Springer, New York, **2006**.

## SUPPORTING INFORMATION

Additional supporting information may be found in the online version of this article at the publisher's website.